ANALYSIS AND COMPENSATION OF NUMERICAL DAMPING IN A ONE DIMENSIONAL AEROELASTIC PROBLEM

Serge Piperno, Bernard Larrouturou
CERMICS
INRIA, 06902 Sophia-Antipolis Cedex, France,

and Michel Lesoinne
Dpt. of Aerospace Engineering Sciences,
Univ. of Colorado at Boulder, Boulder, CO. 80309-429, USA.

Abstract

Here we present analysis methods for a family of staggered schemes that are used in the numerical simulation of fluid-structure interaction problems. The analysis has two goals: to identify the numerical damping errors, in particular those due to the discrete coupling between the fluid and the structure, and to improve the accuracy of the numerical results by compensating these errors. The first analysis method presented is based on the modified equation of the numerical scheme, and the second method is an eigenvector analysis. Both methods provide corrections of the coupled integration schemes in order to eliminate numerical effects, when the system's frequency is known. Other methods are proposed in order to achieve the same goal when this frequency is not known a priori.

ANALYSE ET COMPENSATION DE L'AMORTISSEMENT NUMERIQUE POUR UN PROBLEME AEROELASTIQUE MONO-DIMENSIONNEL

Résumé

Nous présentons ici plusieurs méthodes d'analyse pour des schémas numériques utilisés dans des simulations d'interactions fluide-structure. Le but de cette analyse est double: identifier les erreurs d'origine numérique liées en particulier au couplage entre fluide et structure, et donner un moyen d'éliminer ces effets purement numériques. Nous introduisons deux méthodes d'analyse: la première est fondée sur la théorie des équations équivalentes, et la seconde est une analyse de modes propres. Ces deux méthodes fournissent des corrections des schémas d'intégration du système couplé qui éliminent les effets purements numériques quand la réponse physique du système est connue. D'autres méthodes sont présentées pour les cas où cette réponse est inconnue.

1 Introduction

In aerospace engineering and in the particular field of fluid-structure interaction, it is important to accurately investigate the physical stability of complex coupled systems such as flows around three-dimensional structures [3, 7, 16]. These investigations are performed through numerical simulations [13], in order to better predict the general behaviour of these coupled systems and to prevent unstable phenomena such as flutter or buffetting [4, 9, 15]. Using their own space and time schemes, these simulations naturally have their own stability characteristics [8, 10, 12]. Thus, the results of these simulations give a combination of two responses, the physical one and the numerical one. Of course, it is desirable that the numerical simulation predicts a stable response (respectively: an unstable response) of a physical system only if this system is actually stable (resp.: unstable). Hence, controling the influence of the numerical schemes and in particular of the numerical damping on the numerical results is the only way to reach accuracy, in terms of stability of our numerical simulations.

The ultimate objective of this study is to obtain better integration schemes for fluid-structure interaction problems. For example, the well-known phenomenon of wing flutter corresponds to an unstable behavior of a wing (or a wing-body configuration), which occurs in three-dimensional geometries, with a non-ideal viscous fluid and complex three-dimensional structures. The first step towards better numerical simulations of such phenomena is to analyse simpler fluid-structure problems. This is why we consider in this report numerical simulations of a simple model problem, which we present in Section 2: we deal with a plane piston subjected to the one-dimensional flow of a compressible fluid, in the linear acoustic regime. We use a fixed uniform mesh and take the motion of the piston into account by a boundary mass flux. This formulation allows us to consider a linear problem, which is a necessary first step towards a more complete understanding of fluid-structure interaction. This means also that we have separated here fluid-structure interactions and fluid-mesh interactions (we intend to analyse the latter, which occur in moving meshes methods or ALE-type formulations [2, 5, 6, 8], in a forthcoming work).

Then, the goal of our study is two-fold. Our first goal is to derive methods for obtaining accurate analytical predictions of the general damping of the numerical simulation. Once the first goal is achieved for a large family of schemes, we use these analytical results in order to achieve our second goal, namely modifying the numerical schemes in order to accurately simulate the exact physical damping of the system.

We also present in Section 2 the family of numerical schemes we use: since most engineering coupled applications are simulated with *staggered* schemes (which allow to integrate the structural and the fluid parts separately during each time step), we consider this algorithmic approach. Therefore we use simple schemes for the integration of the fluid and the structure equations. For the boundary conditions, in particular at the fluid-structure boundary, we use different formulations which are commonly used by aeroelasticians; this discrete treatment of the coupling between fluid and structure will appear to have a very strong influence on the numerical results.

In Section 3, we introduce a first method based on the modified equation theory [17] for the numerical analysis of this problem. This method is very simple, and gives good qualitative results provided that the treatment of the boundary conditions is precisely taken into account. These results give useful informations for more general aeroelastic simulations.

In Section 4, we present a more accurate and powerful method for the analysis of the numerical results. This method is based on the analysis of eigenvalues and eigenvectors of the

amplification matrix for the coupled numerical system. Although this method may be uneasily extendable to multi-dimensional cases, it gives in our case very interesting results: it confirms some principles of the common know-how in numerical aeroelasticity, it confirms the results obtained with the modified equation analysis, and it predicts accurately the numerical damping for all linear schemes. The two methods are compared in Section 5.

In Section 6, we discuss applications of both previous methods to different families of schemes. Finally, in Section 7, we show how the results of our analyses can be used more generally for aeroelastic simulations. The presented methods allow us to exactly control the final damping in the numerical simulation when the fundamental frequency of the system is known (which is often the case in aerospatial applications, since flutter pulsations of wing-body configurations are close or equal to eigen-pulsations of the structure). In such a case, we show that we can derive corrections of the numerical schemes in order to compensate the numerical damping. We also propose other general methods for achieving this goal in cases where there is no available a priori evaluation of the system frequency.

2 The physical test case and the global numerical algorithm

In this section, we present the physical experiment under consideration: since actual aerospace engineering problems are too complex to be analysed, we consider a simple one-dimensional model problem. We also present the type of staggering schemes we will use to perform the temporal integration of the coupled fluid-structure system.

2.1 The model problem

We consider the one-dimensional flow of a perfect gas in a chamber closed by a moving piston. The equilibrium state of the system is defined by a uniform pressure P_0 inside and out of the chamber, a uniform gas density ρ_0 in the chamber, where the gas is at rest ($u_0 = 0$), and by a stationnary chamber length L (in our experiment, we take standard values: $P_0 = 1$ atm, $\rho_0 = 1.3$ kg/m^3, $\gamma = 1.4$). The chamber is described on Figure 1.

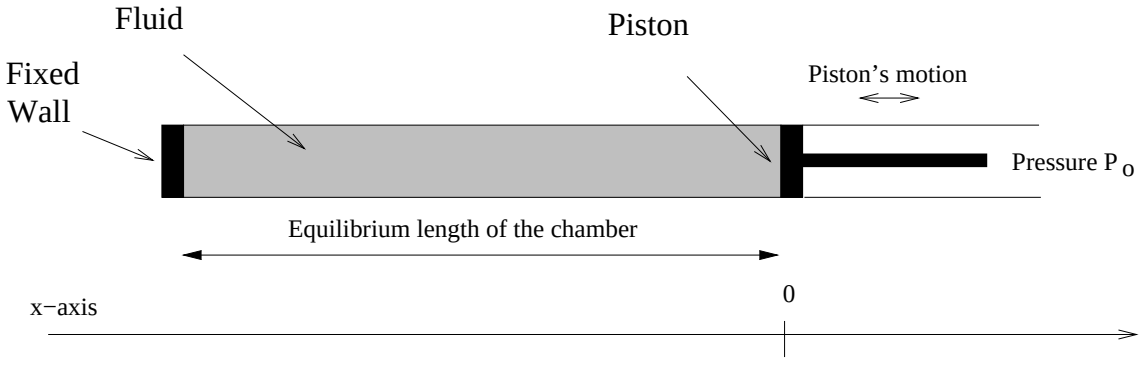

Figure 1: The piston and the fluid-filled one-dimensional chamber.

The one-dimensional flow in the chamber is supposed to be governed by the compressible

Euler equations, which we write with usual notations as:

$$\left\{ \begin{array}{l} \rho_t + (\rho u)_x = 0 \ , \\ (\rho u)_t + (\rho u^2 + P)_x = 0 \ , \\ E_t + [u(E+P)]_x = 0 \ . \end{array} \right. \tag{1}$$

Here, ρ is the density, u is the velocity, P is the pressure and E is the total energy per unit volume. The position, speed and acceleration of the piston are respectively denoted by $L + x$ (i.e. x denotes the deviation of the piston from its equilibrium position), $\dot{x}$ and $\ddot{x}$. Calling m, d and k the mass, the internal damping d and the stiffness of the piston respectively, we write the piston governing equation as:

$$m\ddot{x} + d\dot{x} + kx = P(x+L) - P_0 \ ; \tag{2}$$

here, $P(x+L)$ is the internal pressure at the piston, and we assume that the outer pressure remains constant and equal to P_0.

The boundary conditions for the fluid are:

$$\rho u(0) = 0 \tag{3}$$

at the fixed wall, and:

$$u(x+L) = \dot{x} \tag{4}$$

at the piston, which expresses that the fluid velocity is there equal to the piston speed. Assuming furthermore that the system undergoes only small perturbations around the equilibrium state, we will linearize the above equations. Thus, we assume that:

$$\Delta\rho = \rho - \rho_0 \ \ll \ \rho_0 \ , \tag{5}$$

$$\Delta P = P - P_0 \ \ll \ P_0 \ , \tag{6}$$

$$u \ \ll \ c_0 \ , \tag{7}$$

and, as usual in the linear acoustic regime, we have:

$$\Delta P = c^2 \Delta\rho \ , \tag{8}$$

which means that the gas variations are isentropic (we simply denote by c instead of c_0 the unperturbed sound speed). We then write the governing equations using the vector $W = \begin{pmatrix} \Delta\rho \\ \Delta(\rho u) \end{pmatrix} = \begin{pmatrix} \Delta\rho \\ \rho_0 \Delta u \end{pmatrix}$ as:

$$W_t + \begin{pmatrix} 0 & 1 \\ c^2 & 0 \end{pmatrix} W_x = 0 \ . \tag{9}$$

The linearized boundary conditions take the form:

$$\Delta u(0) = 0 \ , \tag{10}$$

$$\Delta u(L) = \dot{x} \ , \tag{11}$$

and the piston equation now can be written as:

$$m\ddot{x} + d\dot{x} + kx = \Delta P(L) = c^2 \Delta\rho(L) \ . \tag{12}$$

2.2 Evaluating the system frequency

In the following, the reader will assume that d and k are equal to 0, if no other explicit statement is made. The piston equation then reduces to:

$$m\ddot{x} = \Delta P(L) = c^2 \Delta\rho(L) \; . \tag{13}$$

Since d is equal to 0, the physical system is undamped and should undergo infinite oscillations of constant amplitude. We now present two different ways of evaluating the frequency of these oscillations.

The first crude estimate can be obtained in a very simple and rapid way by assuming that, in addition to being isentropic, the gas flow is isobaric. In other words, one assumes that the pressure is spatially constant in the chamber (an assumption which is consistent with the highly subsonic character of the flow). Using this approximation (which differs from the acoustic approximation described above), we can write:

$$m\,\ddot{x} = P - P_0, \tag{14}$$

where $P = P(t)$ is the spatially constant pressure. It is given by:

$$P\rho^{-\gamma} = P_0{\rho_0}^{-\gamma} \; , \tag{15}$$

where ρ is the gas density (also spatially constant). Writing the mass conservation for the system, we have:

$$(L + x)\,\rho = L\,\rho_0. \tag{16}$$

The position x then satisfies the following equation:

$$m\,\ddot{x} = P_0 \left[\left(\frac{L+x}{L} \right)^{-\gamma} - 1 \right]. \tag{17}$$

For small enough initial perturbations (in piston speed and location), we can linearize the preceding equation for $x \ll L$. We get:

$$m\,\ddot{x} = -\frac{\gamma P_0}{L} x. \tag{18}$$

Hence, the "isobaric pulsation" ω_i of the system is given by:

$${\omega_i}^2 = \frac{\gamma P_0}{mL}. \tag{19}$$

This formula can be rewritten with dimensionless quantities as

$$\boxed{\left(\frac{\omega_i L}{c} \right)^2 = \frac{\rho_0 L}{m}.} \tag{20}$$

Now, a second more instructive way of evaluating the system frequency consists in solving the linear system (9)-(13). Indeed, a major interest of this one-dimensional acoustic physical experiment is that we can exhibit an exact solution of the linear system (9)-(13). This exact solution will be used later for more complex predictions. We have the following:

Lemma 1 *A solution of equation (9) with the boundary condition (10) is given by:*

$$W = \begin{pmatrix} 1 \\ +c \end{pmatrix} \cos[\omega(t - \frac{x}{c})] + \begin{pmatrix} 1 \\ -c \end{pmatrix} \cos[\omega(t + \frac{x}{c})] \quad (\text{with } \omega \in I\!R). \tag{21}$$

The proof is elementary and will be omitted.

In order to solve the complete system (9)-(13), it remains to take into account the piston boundary condition (11) and the equation (13) for the piston dynamics. Using (21), we then have:

$$u(L) = -\frac{2c}{\rho_0} \sin(\frac{\omega L}{c}) \sin(\omega t) \ , \tag{22}$$

$$m\dot{u}(L) = \frac{2mc\omega}{\rho_0} \sin(\frac{\omega L}{c}) \cos(\omega t) \ , \tag{23}$$

$$\Delta P(L) = 2c^2 \cos(\frac{\omega L}{c}) \cos(\omega t) \ . \tag{24}$$

Hence, the piston equation (13) is satisfied if and only if:

$$\frac{2mc\omega}{\rho_0} \sin(\frac{\omega L}{c}) = 2c^2 \cos(\frac{\omega L}{c}) \ , \tag{25}$$

which can be written as

$$\boxed{\left(\frac{\omega L}{c}\right) \tan\left(\frac{\omega L}{c}\right) = \frac{\rho_0 L}{m}.} \tag{26}$$

This formula deserves several comments. First, this relation is consistent with the previous "isobaric estimate" (20): in the limit of c going to $+\infty$, then $\tan(\omega L/c) \simeq \omega L/c$ and ω tends to ω_i.

Also, two interesting limits can be observed for relation (26). If m tends to $+\infty$, then $\frac{\omega L}{c} = k\pi$: the infinite-mass piston behaves as a fixed wall, and we have a classical acoustic regime with a velocity node at each end of the chamber. On the other hand, if m tends to 0, then $\frac{\omega L}{c} = \frac{\pi}{2} + k\pi$: the boundary condition at the piston becomes $\Delta P(L) = 0$ from (13), and we now have an acoustic regime with a velocity node at the fixed wall and a pressure node a the piston.

Beside this, since $\tan(z) > z, \forall z \in]0, \pi/2[$, we see that the fundamental pulsation given by (26) is smaller than ω_i. Thus, the period of the system is greater than the "isobaric period", which is also coherent with the hypothesis of finite wave speed.

2.3 The general integration scheme

We conclude this section by briefly presenting the general type of schemes used in our simulations below. The algorithm is derived from general aeroelasticity know-how [12, 13] and uses so-called staggering schemes, where the fluid and the structure are integrated separately during each time step.

Thus, the algorithm is the following: at each time level t^n, we:

- predict the piston speed for the next time step $[t_n, t_{n+1}]$,
- compute wall fluxes for the fluid during this time step,
- integrate the fluid from t_n to t_{n+1},
- compute an average pressure at the piston for the time step $[t_n, t_{n+1}]$,
- integrate the piston (submitted to this pressure) from t_n to t_{n+1}.

We notice here that we could have used other staggering schemes, where the structure is integrated first. But in fact, these algorithms differ only by indices translations.

In the following, we consider only explicit time integration schemes (except in section 6.3 below).

Although we postpone till the end of this report the presentation of our numerical results for the oscillating piston, it is worth saying here that the clearest feature of these result lies in the inability of the numerical schemes to reproduce the constant-amplitude system oscillations: the amplitude of the computed oscillations decreases with time (see e.g. Figure 2 below). Moreover, we sometimes also observe a deviation between the computed frequency and the known analytical frequency. Analysing these numerical effects, and in particular the numerical damping, is the object of the next sections.

3 Modified equation analysis

In this section, we use the modified equation theory [17] to obtain analytical predictions of our numerical results. Referring to [1, 17] for the details, we simply recall here that, for the numerical solution of a linear hyperbolic or parabolic equation, the modified equation is the differential equation which is exactly satisfied by the computational values; it is obtained through Taylor expansions, and it is an adequate way to express the main properties of the numerical schemes, in terms of error analysis.

Let us recall the following example, which will be useful later on. Consider the numerical solution of the advection equation $u_t + cu_x = 0$, with $c > 0$, with the simple explicit upwind scheme:

$$\frac{u_j^{n+1} - u_j^n}{\Delta t} + c\frac{u_j^n - u_{j-1}^n}{\Delta x} = 0 \ . \tag{27}$$

Then, the modified equation of this scheme is, up to second order accuracy (see e.g. [1]):

$$u_t + cu_x = \mu u_{xx} + c\lambda u_{xxx} \ , \tag{28}$$

with:

$$\mu = \frac{c\Delta x}{2}(1-\nu) \ , \tag{29}$$

$$\lambda = -\frac{\Delta x^2}{6}\left(1-3\nu+2\nu^2\right) \ , \tag{30}$$

where the Courant number ν is given by $\nu = \dfrac{c\Delta t}{\Delta x}$.

Recalling that out goal is to analyse the numerical errors for the coupled fluid-structure system, we are going to use the modified equation in order to represent the numerical errors related to the simulation of the fluid (more precisely, of the linear acoustic waves in the fluid). We will therefore have to couple the modified equation with the discrete piston equation, and we will see that not only the numerical approximation in the fluid (taken into account through the modified equation), but also the time integration scheme for the structure and the discrete treatment of boundary conditions have important influences on the numerical results.

3.1 Modified equation with diffusion

Let us assume that we use an explicit first-order accurate upwind scheme for the integration of system (9). Restricting our attention to the main error term in the fluid approximation, we will consider that our numerical solution satisfies:

$$W_t + \begin{pmatrix} 0 & 1 \\ c^2 & 0 \end{pmatrix} W_x = \mu W_{xx} \ , \tag{31}$$

where the positive diffusion coefficient μ is given in (29).

Since this equation differs from (9), we are now interested in appreciating the influence of μ on the system pulsation. We will use the same method as in the undamped case. The essential difference lies in finding elementary solutions of (31). The first natural idea consists in taking temporally damped oscillations. With this kind of solution, it is not possible to fulfill both the fixed wall boundary condition (10) and the fundamental equation of dynamics for the piston. Thus, we will consider temporally and spatially damped oscillations:

Lemma 2 *A solution of equation (31) with the boundary condition (10) is given by:*

$$W = e^{z(\mu z - c)t}\left[\begin{pmatrix} 1 \\ +c \end{pmatrix} e^{zx} + \begin{pmatrix} 1 \\ -c \end{pmatrix} e^{-zx}\right] \quad (\text{with } z \in \mathbf{C}). \tag{32}$$

We leave the proof to the reader.

As previously, we can write:

$$u(L) = \frac{2c}{\rho_0}\sinh(zL)e^{z(\mu z-c)t} \ , \tag{33}$$

$$m\dot{u}(L) = \frac{2mc}{\rho_0}\sinh(zL)z(\mu z - c)e^{z(\mu z-c)t} \ , \tag{34}$$

$$\Delta P(L) = 2c^2\cosh(zL)e^{z(\mu z-c)t} \ . \tag{35}$$

Hence, the fundamental equation (13) is satisfied if and only if:

$$\frac{2mc}{\rho_0}\sinh(zL)z(\mu z - c) = 2c^2\cosh(zL)\ , \tag{36}$$

which can be written as:

$$z(\mu z - c)\tanh(zL) = \frac{\rho_0 c}{m}\ , \tag{37}$$

or:

$$\boxed{(-izL)\left(1 - \frac{\mu z}{c}\right)\tan(-izL) = \frac{\rho_0 L}{m}\ .} \tag{38}$$

Equation (38) has conjugate solutions. It is consistent with (26): indeed, if we take $\mu = 0$ in (38), it can be proved that $z = \pm\dfrac{i\omega}{c}$, with ω given by (26) (the reader may check that a complex number r such that $r\tan(r) \in I\!R^+$ is necessarily on the imaginary axis).

Remark 1: Before analyzing the relation (38), let us come back to (31), and investigate whether it was valid to keep only the diffusion error term. If we add the dispersion term, we write, up to second order in Δx and Δt:

$$W_t + \begin{pmatrix} 0 & 1 \\ c^2 & 0 \end{pmatrix} W_x = \mu W_{xx} + \lambda \begin{pmatrix} 0 & 1 \\ c^2 & 0 \end{pmatrix} W_{xxx}\ , \tag{39}$$

where the dispersion coefficient λ is given by (30). As above for Lemma 2, we can show that the elementary solutions of equation (39) with the boundary condition (10) are given by:

$$W = e^{z(\mu z - c + \lambda c z^2)t}\left[\begin{pmatrix} 1 \\ +c \end{pmatrix} e^{zx} + \begin{pmatrix} 1 \\ -c \end{pmatrix} e^{-zx}\right] \quad (\text{for } z \in \mathbf{C}). \tag{40}$$

Then, the equation (38) for z becomes:

$$\frac{2mc}{\rho_0}\sinh(zL)z(\mu z - c + \lambda c z^2) = 2c^2\cosh(zL)\ . \tag{41}$$

Of course, the preceding equation reduces to (38) when $\lambda = 0$. But we see also that the influence of the dispersion term is much weaker than the one of the diffusion term, since the ratio $\dfrac{\lambda c z^2}{\mu z}$ is small (when μ and λ are small, i.e. for $z \approx \pm\dfrac{i\omega}{c}$):

$$\frac{|\lambda c z^2|}{|\mu z|} = \left(\frac{1 - 2\nu}{3}\right)\frac{\omega\Delta x}{c}\ . \tag{42}$$

Therefore, we will actually neglect the dispersion error in the sequel, and analyse equation (38) instead of (41). •

It is also interesting to analyse the dependence of the solution z of (38) on the diffusion parameter μ. We can linearize the equation for z around $\mu = 0$, knowing that for $\mu = 0$, $z = \pm\dfrac{i\omega}{c}$. We obtain (the details are omitted):

$$\left.\frac{\partial I\!m\left(z(\mu z - c)\right)}{\partial\mu}\right|_{\substack{\mu=0 \\ z=\pm i\omega/c}} = 0\ , \tag{43}$$

$$\left.\frac{\partial \mathcal{R}e\left(z(\mu z - c)\right)}{\partial \mu}\right|_{\substack{\mu=0 \\ z=\pm i\omega/c}} = -\frac{\omega^2}{c^2}\left[1 - \left[1 + \frac{\rho_0 L}{m}\left(1 + \frac{m^2\omega^2}{\rho_0^2 c^2}\right)\right]^{-1}\right] \ . \tag{44}$$

Thus, from (43), it follows that the temporal pulsation of the elementary waves are changed only at the second order when μ is small (recall from Lemma 2 that $z(\mu z - c)$ is precisely the coefficient of the time variable t in the solution (32)).

The interpretation of (44) is less obvious. For the sake of convenience, we have considered so far complex variables, but we should now come back to the actual (real) variables, and observe the actual piston motion. With our complex solution, we have $\dot{x} = \dfrac{2c}{\rho_0}\sinh(zL)e^{z(\mu z - c)t}$, whence $x = \dfrac{2c}{a\rho_0}\sinh(zL)e^{at}$, with $a = z(\mu z - c)$. Then, it is easy to check that we can write an equation of the form:

$$m\ddot{x} = \alpha x + \beta \dot{x} \tag{45}$$

for the piston, with α and β real, by taking:

$$\alpha = -m|a|^2 = -m|z(\mu z - c)|^2 \ , \quad \beta = 2m\mathcal{R}e(a) = 2m\mathcal{R}e\left(z(\mu z - c)\right) \ . \tag{46}$$

Thus, we are now able to know the stiffness and the damping induced by the fluid on the piston. For $\mu = 0$, we find of course $\alpha = -m\omega^2$ and $\beta = 0$. For a small diffusion μ, we get from (43) and (44):

$$\beta = -\frac{2m\omega^2}{c^2}\left[1 - \left[1 + \frac{\rho_0 L}{m}\left(1 + \frac{m^2\omega^2}{\rho_0^2 c^2}\right)\right]^{-1}\right] \mu + O(\mu^2) \ , \tag{47}$$

$$\alpha = -m\omega^2 + O(\mu^2) \ . \tag{48}$$

$$\tag{49}$$

Remark 2: We achieved the same study with retaining the second-order terms (but still neglecting the dispersion term in the modified equation). It shows that no second-order term is introduced in the expansion of the damping β by the diffusion μ. The influence of the dispersion error will be analysed with second-order accurate schemes in Section 6.2 below. •

3.2 Roles of the scheme for the structure and of the discrete boundary conditions

Through α and β, the above analysis predicts analytical values for the numerically observed pulsation and damping of the piston oscillations. For the pulsation of the coupled system, the prediction (26) reveals to compare very well with numerical simulations: it gives a predicted pulsation with a relative error less than one percent. This great accuracy is partly explained by (48). But the analytically predicted damping factor β is not so accurate and is even sometimes quite far from the numerical results.

In the following, we give explanations for this inaccuracy of the above analysis. We will derive a new formula for the numerical damping β of the system, and we will check the validity of the preceding prediction for α.

3.2.1 Sources of numerical damping

In the physical problem, we did not introduce any dissipation which could produce damping ($d = 0$ in (12)). The whole damping is therefore of numerical origin. The first origin lies in the numerical scheme for the fluid, and was taken into account through the modified equation. But there is a second origin of numerical dissipation, which is related to the temporal integration of the piston's motion.

Indeed, in the above analysis, we considered that the numerical solution W in the fluid is no longer discrete, but continuous in space and time: it is the solution (32) of the modified equation (31), and we considered that all spatial and temporal errors of the fluid approximation are dealt with through the modified equation. However, we also used a time-continuous representation for the piston, since we coupled the solution (32) with the differential piston equation (13). In practice, in the numerical simulations, we use a discrete form of the fundamental equation, and the numerical errors related to this approximation have been neglected in the above analysis, since they are not taken into account in the modified equation of the fluid.

For instance, if the speed of the piston is computed with the scheme:

$$m\frac{\dot{x}^{n+1} - \dot{x}^n}{\Delta t} = \Delta P^n(L) \ , \tag{50}$$

then the argument used in the preceding section to obtain equations (36) and (38) is no longer valid. We then have to introduce the discrete temporal scheme in our reasoning.

3.2.2 New predictions for the numerical damping

Let us therefore come back to (32), and search a new equation for z, assuming that the scheme (50) is used for the piston. From (33) and (35), we deduce (still denoting $a = z(\mu z - c)$):

$$m\frac{e^{a\Delta t} - 1}{\Delta t}\frac{2c}{\rho_0}\sinh(zL) = 2c^2\cosh(zL) \ , \tag{51}$$

which can be rewritten as:

$$z(\mu z - c)\tanh(zL) = \frac{\rho_0 c}{m}\frac{a\Delta t}{e^{a\Delta t} - 1} \ , \tag{52}$$

which now replaces (37).

The expansion of z around the value $z_0 = \pm\dfrac{i\omega}{c}$ (where ω is given by (26)) in terms of μ and Δt (which are assumed to be small with respect to c^2/ω and $1/\omega$ respectively) takes the form:

$$z = \pm\frac{i\omega}{c} - \left[1 + \frac{\rho_0 L}{m}\left(1 + \frac{m^2\omega^2}{\rho_0^2 c^2}\right)\right]^{-1}\left[\frac{\omega^2}{c^3}\mu + \frac{\omega^2}{2c}\Delta t\right] , \tag{53}$$

hence:

$$\boxed{\begin{aligned}\beta \ = \ & -\frac{2m\omega^2}{c^2}\left[1 - \left[1 + \frac{\rho_0 L}{m}\left(1 + \frac{m^2\omega^2}{\rho_0^2 c^2}\right)\right]^{-1}\right]\mu \\ & + m\omega^2\left[1 + \frac{\rho_0 L}{m}\left(1 + \frac{m^2\omega^2}{\rho_0^2 c^2}\right)\right]^{-1}\Delta t \\ & + O(\mu^2, \Delta t^2) \ .\end{aligned}} \tag{54}$$

The preceding formula appears to give a very good prediction of the total numerical damping. For example, we simulated the motion of a 0.8kg piston with a one meter chamber, and tried several values of the Courant number (with 50 mesh points). With $\nu = 0.045$, we numerically found $\beta = -1.87$, whereas our formula (54) predicts $\beta = -1.80$. For $\nu = 0.45$, we found $\beta = -1.33$ and the analytical prediction is $\beta = -1.32$. The average error is then less than 4% in the first case, less than 1% in the latter.

4 Coupled eigenvector analysis

In the previous section, we were only able to take partially into account the influence of the discrete treatment of the boundary conditions on the numerical simulations. We now have to be more specific about these conditions, and analyse in details their overall effect on the numerical damping of the piston oscillations.

To be more specific, let us write down the boundary conditions for the family of schemes considered in this section. We call N the number of computational cells in the chamber $[0, L]$ (i.e. $N\Delta x = L$), and write the explicit scheme under the following form, for $1 \leq i \leq N$:

$$\frac{W_i^{n+1} - W_i^n}{\Delta t} + \frac{\Phi_{i+1/2}^n - \Phi_{i-1/2}^n}{\Delta x} = 0 \ . \tag{55}$$

Outside the boundaries, the numerical flux $\Phi_{i+1/2}^n$ is based on first-order upwinding. For $\Phi_{1/2}^n$, at the fixed wall, we use upwinding with a "mirror" cell, i.e. a fictitious cell with the same density as in the first cell and the opposite momentum of the first true cell. At the other end of the chamber, we have to evaluate a flux through the moving piston; we take:

$$\Phi_{N+1/2}^n = \begin{pmatrix} \rho_0 V_p^* \\ c^2 \Delta\rho_N^n \end{pmatrix} \ . \tag{56}$$

Here, V_p^* is a prediction of the piston speed, evaluated as a weighted average of the n^{th} and $n+1^{st}$ computational speeds by the formulas:

$$m\frac{V_p^{n+1} - V_p^n}{\Delta t} = c^2 \Delta\rho_N^n \ , \tag{57}$$

$$V_p^* = (1-\theta)V_p^n + \theta V_p^{n+1} \ , \tag{58}$$

where θ is a fixed parameter. Such conditions are commonly used in aeroelasticity simulations (see e.g. [7]).

At first sight, we are not able to really take these conditions into acount in the modified equation analysis of the previous section. This is why we now introduce a second method, which we call the "coupled eigenvector analysis".

4.1 Presentation of the analysis

The analysis which we now present is an eigenvector and eigenvalues analysis. We consider the set of all computational values at a certain time step, for both the fluid and the piston, and

we see it as an unknown vector which is changing during time integration. We still denote by W the vector of the conserved variables for the fluid and by V_p the speed of the piston. Let us also add that we still consider the physically undamped and free (i.e. with no spring) piston ($d = k = 0$ in (12)).

Writing the complete scheme under the form:

$$\begin{pmatrix} W \\ V_p \end{pmatrix}^{n+1} = \begin{pmatrix} W \\ V_p \end{pmatrix}^{n} + \Delta t \mathcal{F} \begin{pmatrix} W \\ V_p \end{pmatrix}^{n}, \tag{59}$$

we are going to search the eigenvectors and eigenvalues of the linear operator $\mathcal{F}$, which in particular takes into account the detailed formulation of the discrete coupling between fluid and structure.

From our knowledge of the exact solution (21) and of the modified solution (32), we may make a good guess for the eigenvectors of the coupled operator $\mathcal{F}$. We set:

$$\left\{ \begin{array}{rcl} W_1^n &=& A^n W^+ e^{z x_1} + k^g \; B^n W^- e^{-z x_1} \;, \\ W_i^n &=& A^n W^+ e^{z x_i} + B^n W^- e^{-z x_i} \quad \text{for } 1 < i < N \;, \\ W_N^n &=& k^d \; A^n W^+ e^{z x_N} + B^n W^- e^{-z x_N} \;, \end{array} \right. \tag{60}$$

where $x_i = \left(i - \dfrac{1}{2}\right) \Delta x$ is the center of the th cell, $z \in \mathbf{C}$ is a spatial pulsation, $W^{\pm} = \begin{pmatrix} 1 \\ \pm c \end{pmatrix}$ are the eigenvectors of the acoustic matrix appearing in (9), A^n and B^n are the amplitudes of the forward and backward waves, k_g and k_d are correction coefficients at both ends of the chamber.

Our goal is to find A^n, B^n, k_g, k_d and z such that:

1. the solution at time $t^{n+1} = t^n + \Delta t$ has the form:

$$\left\{ \begin{array}{rcl} W_1^{n+1} &=& A^{n+1} W^+ e^{z x_1} + k^g \; B^{n+1} W^- e^{-z x_1} \;, \\ W_i^{n+1} &=& A^{n+1} W^+ e^{z x_i} + B^{n+1} W^- e^{-z x_i} \quad \text{for } 1 < i < N \;, \\ W_N^{n+1} &=& k^d \; A^{n+1} W^+ e^{z x_N} + B^{n+1} W^- e^{-z x_N} \;; \end{array} \right. \tag{61}$$

2. there exists a complex number λ such that:

$$\frac{A^{n+1}}{A^n} = \frac{B^{n+1}}{B^n} = \frac{V_p^{n+1}}{V_p^n} = \lambda \;. \tag{62}$$

4.2 Coupled eigenvector analysis with a predicted piston speed

Let us conduct this eigenvector analysis, for the scheme detailed in equations (55)-(58). We give the main outlines of the whole computation. First we write the evolution equation for the fluid in a medium cell (including cells 2 and $N-1$, because the upwind fluxes for these cells do not involve neither k_g nor k_d). Writing $x = x_i$, for $2 \leq i \leq N-1$, we have:

$$W_i^{n+1} = W_i^n + \frac{\Delta t}{\Delta x} \left[c A^n W^+ e^{z(x-\Delta x)} - c B^n W^- e^{-zx} - c A^n W^+ e^{zx} + c B^n W^- e^{-z(x+\Delta x)} \right] \;. \tag{63}$$

Identifying with (62), we get:

$$\frac{A^{n+1}}{A^n} = \frac{B^{n+1}}{B^n} = 1 + \frac{c\Delta t}{\Delta x}\left(e^{-z\Delta x} - 1\right) = \lambda \ . \tag{64}$$

If we write the same equation for the first cell, we obtain:

$$W_1^{n+1} = W_1^n + \frac{\Delta t}{\Delta x}\left[c\left(W^+ - W^-\right)k_g B^n e^{-zx_1} - cA^n W^+ e^{zx_1} + cB^n W^- e^{-z(x_1+\Delta x)}\right] \ , \tag{65}$$

and the identification implies:

$$k_g = 1 \ , \tag{66}$$

$$B^n = A^n \ . \tag{67}$$

The equation for the last cell writes:

$$\begin{aligned} W_N^{n+1} = W_N^n + \frac{\Delta t}{\Delta x}[\quad & cA^n W^+ e^{z(x_N-\Delta x)} - cB^n W^- e^{-zx_N} \\ & -\frac{\rho_0 V_p^*}{2}\left(W^+ + W^-\right) - \frac{c\Delta\rho_N^n}{2}\left(W^+ - W^-\right)\ ] \ . \end{aligned} \tag{68}$$

Introducing the expressions of V_p^* and $\Delta\rho_N^n$, the preceding equation implies:

$$k_d = 1 + \left(1 - e^{z\Delta x}\right)e^{-2zx_N} \ , \tag{69}$$

$$\begin{aligned} \frac{V_p^n}{A^n} = & -\frac{c^2\theta\Delta t}{m}\left[2\cosh zx_N + \left(1 - e^{z\Delta x}\right)e^{-zx_N}\right] \\ & -\frac{2c}{\rho_0}\left[e^{-zx_N}\left(e^{-z\Delta x} - 1\right) - \frac{1}{2}\left(e^{zx_N} - e^{-zx_N}e^{z\Delta x}\right)\right] \ . \end{aligned} \tag{70}$$

Lastly, writing the last relation (62), we find an additional equation which determines z (and therefore λ from (64)):

$$\boxed{\begin{aligned} \frac{1}{m}\left[\frac{\Delta x}{(e^{-z\Delta x} - 1)} + \theta c\Delta t\right] \quad & \left[2\cosh zx_N + \left(1 - e^{z\Delta x}\right)e^{-zx_N}\right] = \\ -\frac{2}{\rho_0} \quad & \left[e^{-zx_N}\left(e^{-z\Delta x} - 1\right) - \sinh zx_N + \frac{1}{2}e^{-zx_N}\left(e^{z\Delta x} - 1\right)\right] \ . \end{aligned}} \tag{71}$$

We recall that, in this equation, x_N is given by $x_N = L - \Delta x/2$. Notice also that, as expected, the amplitudes A_n, B_n are determined only up to a multiplicative constant.

Equation (71) is very interesting. For example, *if we assume that* $\theta = 0$ and if we take the limit when Δt and Δx tend to 0, we find exactly equation (26).

Assuming that Δx and Δt are very small (compared with c/ω and $1/\omega$ respectively), we can obtain the following expansion of z around the value $z_0 = \pm\dfrac{i\omega}{c}$ given by (26):

$$z = z_0 - \frac{\omega^2}{2c^2}\left[1 + \frac{\rho_0 L}{m}\left(1 + \frac{m^2\omega^2}{\rho_0^2 c^2}\right)\right]^{-1}\left[\Delta x - 2\theta c\Delta t\right] \ . \tag{72}$$

Defining the coefficient a by setting $\lambda = \exp(a\Delta t)$, we can again define the stiffness coefficient α and the continuous damping β as in (46). Then α can be shown to be equal to its previous value $\alpha = -m\omega^2$ up to second-order accuracy, whereas, using (64) and (72), we find:

$$\boxed{\frac{\beta}{2m} = \frac{\omega^2(\nu-1)\Delta x}{2c} - \frac{\omega^2(2\theta\nu-1)\Delta x}{2c\left[1+\dfrac{\rho_0 L}{m}\left(1+\dfrac{m^2\omega^2}{\rho_0^2 c^2}\right)\right]}\ .} \tag{73}$$

Thus, we now have a precise analytical prediction of the numerical damping effect, which takes into account in full detail the numerical formulation (55)-(58). The question is then to compare this prediction with the prediction (54) obtained with the modified equation analysis.

5 Comparing the two methods

The first remark to be pointed out about equation (73) is the following one: if we take $\theta = 0$, corresponding to the choice $V_p^* = V_p^n$ in (58), we find exactly the same prediction for β as in (54) (with μ in (54) given by (29)). This is the reason why our previous prediction (54) turned out to be valid when we took $V_p^* = V_p^n$, as in the simulations whose results are reported at the very end of Section 3.

Now, if we take $\theta \neq 0$ in (73), we find a different prediction. Again, this analytical prediction revealed to be very accurate when compared with the actually observed damping of the piston in a numerical simulation: for the same physical parameters as before but with $\theta = 1$, the simulation gave $\beta = -2.73$, whereas (73) predicts $\beta = -2.82$, i.e. the error in the prediction is again less than 4%.

It is also worth noticing that, when $\theta > 0$, $\beta < \beta_{\theta=0}$. Taking a positive value for θ gives more damping and more stable numerical simulations. This explains the usual choice of aeroelasticians.

At this point, we may wonder whether the modified equation analysis is really restricted to cases where $\theta = 0$: is it really impossible to analyse the schemes operating with $\theta \neq 0$ using the modified equation analysis? This question leads us to revisit our first analysis, and will also allow us to better understand the equations (57)-(58).

Indeed, for the modified equation analysis, we did not explicitly describe the discrete boundary condition at the piston. Of course, the treatment of the boundary has no influence on the modified equation itself, which concerns only the internal part of the flow. But, in practice, the formulation of the boundary condition with the parameter θ induces a certain time shift between the fluid and the structure, and this acts as a modified boundary condition for the modified equation.

Let us be more specific, and show how we can handle the dependence on θ within the modified equation analysis. To make the boundary flux (56) consistent with the other numerical fluxes, we have to consider that V_p^* is an approximation of the piston speed at time $n\Delta t$. But then, from (58), the n^{th} computational piston speed V_p^n represents the speed of the piston at time $(n-\theta)\Delta t$! In other words, for the scheme (55)-(58) with the parameter θ, we should replace equation (50) in the modified equation analysis by:

$$m\frac{\dot{x}[(n+1-\theta)\Delta t] - \dot{x}[(n-\theta)\Delta t]}{\Delta t} = \Delta P(L, n\Delta t)\ . \tag{74}$$

Instead of (51), we then find:

$$me^{-a\theta\Delta t}\frac{e^{a\Delta t}-1}{\Delta t}\frac{2c}{\rho_0}\sinh(zL)=2c^2\cosh(zL)\ , \tag{75}$$

and the final result for β, which replaces (54), becomes:

$$\boxed{\beta=-\frac{2m\omega^2\mu}{c^2}+\frac{m\omega^2\left(\frac{2\mu}{c^2}+(1-2\theta)\Delta t\right)}{\left[1+\frac{\rho_0 L}{m}\left(1+\frac{m^2\omega^2}{\rho_0^2c^2}\right)\right]}++O(\mu^2,\Delta t^2)\ .} \tag{76}$$

It is straightforward to see that this prediction exactly coincides with (73) (again with the value (29) of μ). We have therefore extended the modified equation analysis to the above family of schemes, for any value of the parameter θ, and we have also learnt how to interprete the role of this parameter: V_p^* is an approximation of the piston speed at time $n\Delta t$, and V_p^n must be seen as an evaluation of the piston speed at time $(n-\theta)\Delta t$.

Remark 3: Since the modified equation analysis is easier to conduct than the eigenvector analysis, the preceding remarks about the extension of the former make it possible to analyse situations where the eigenvector analysis would be very complex or would even fail, because finding the analytical form of the eigenvectors is impossible. For example, we simulated a slightly different problem, with acoustic waves propagating in a chamber of fixed length L (without a piston), but moving on tracks without friction. The coupled eigenvector analysis is feasible but complex. On the contrary, it is easy to solve the modified equation; we find that:

$$W=\left[W^+e^{zx}-W^-e^{z(L-x)}\right]e^{z(\mu z-c)t}\ . \tag{77}$$

For the "θ-scheme" (i.e. with discrete equations similar to (57)-(58) for the chamber velocity), the complex pulsation z is solution of:

$$e^{-a\theta\Delta t}\frac{e^{a\Delta t}-1}{\Delta t}=\tanh(\frac{zL}{2})\frac{2c\rho_0}{m}\ . \tag{78}$$

Then, the new pulsation $\bar\omega$ and the new damping $\bar\beta$ are given by:

$$\tan(\frac{\bar\omega L}{2c})=-\frac{m}{\rho_0 L}\frac{\bar\omega L}{2c}\ , \tag{79}$$

and:

$$\boxed{\frac{\bar\beta}{2m}=\frac{\bar\omega^2(\nu-1)\Delta x}{2c}-\frac{\bar\omega^2(2\theta\nu-1)\Delta x}{2c\left[1+\frac{\rho_0 L}{m}\left(1+\frac{m^2\bar\omega^2}{4\rho_0^2c^2}\right)\right]}\ .} \tag{80}$$

These predictions were numerically tested and we again found an error less than 3%. Moreover, we also performed artificially undamped solutions of the physical problem with an adequate value of θ (see Section 7.2 below). •

6 Analysing other schemes

We now use the two previous methods in order to analyse some other schemes for our model fluid-structure problem.

6.1 Schemes with predicted pressure and speed

In this part, we conduct the coupled eigenvector analysis for other schemes which are also commonly used by aeroelasticians, where a predicted pressure at the piston is used. Instead of (56), we now use a wall flux given by:

$$\Phi^n_{N+1/2} = \begin{pmatrix} \rho_0 V_p^* \\ c^2 \Delta\rho^* \end{pmatrix} \ , \tag{81}$$

with:

$$\Delta\rho^* = (1-\phi)\,\Delta\rho^n_N + \phi \Delta\rho^{n+1}_N \ , \tag{82}$$

where $\Delta\rho^{n+1}_N$ is predicted with the first component of (68). The predicted piston speed V_p^* is still given by (57)-(58).

The computation follows the same lines as above. Equations (64), (66) and (67) still hold, and the evolution equations for the solution in the last cell gives:

$$\Delta\rho^{n+1}_N = \Delta\rho^n_N + \frac{\Delta t}{\Delta x}\left[cA^n e^{z(x_N-\Delta x)} - cB^n e^{-zx_N} - \rho_0 V^*\right] \ , \tag{83}$$

$$\Delta(\rho u)^{n+1}_N = \Delta(\rho u)^n_N + \frac{c\Delta t}{\Delta x}\left[cA^n e^{z(x_N-\Delta x)} + cB^n e^{-zx_N} - c\Delta\rho^*_N\right] \ . \tag{84}$$

Introducing the expressions of V^* and $\Delta\rho^*$, we deduce from the preceding equations (after a quite heavy computation) that:

$$k_d = \frac{1 + e^{-2zx_N}\left(1-e^{z\Delta x}\right)\left(1-\dfrac{c\phi\Delta t}{\Delta x}\right)}{1+\left(1-e^{z\Delta x}\right)\dfrac{c\phi\Delta t}{\Delta x}} \ , \tag{85}$$

$$\frac{V^n_p}{A^n} = -\frac{c}{\rho_0}\left[\left(e^{-z\Delta x} - 1 + \frac{\rho_0 c\theta\Delta t}{m}\right)\left(k_d e^{zx_N} + e^{-zx_N}\right) + e^{-zx_N} - e^{z(x_N-\Delta x)}\right] \ . \tag{86}$$

Using (57) and the last equality in (62), we finally obtain the following relation fixing z:

$$\boxed{\left[\frac{\rho_0\Delta x}{m\left(e^{-z\Delta x}-1\right)} + e^{-z\Delta x} - 1 + \frac{\rho_0 c\theta\Delta t}{m}\right]\left[k_d e^{zx_N} + e^{-zx_N}\right] = e^{z(x_N-\Delta x)} - e^{-zx_N} \ .} \tag{87}$$

Assuming again that Δx and Δt are very small (respectively compared with c/ω and $1/\omega$), we can obtain the new expansion of z around the value $z_0 = \pm\dfrac{i\omega}{c}$. We first find:

$$k_d = 1 + z_0\left(1+e^{-2Lz_0}\right)\left(c\phi\Delta t - \Delta x\right) \ , \tag{88}$$

whence:

$$z = z_0 - \frac{\omega^2}{2c^2}\left[1 + \frac{\rho_0 L}{m}\left(1 + \frac{m^2\omega^2}{\rho_0^2 c^2}\right)\right]^{-1} [\Delta x - 2(\theta - \phi)c\Delta t] \ . \tag{89}$$

Using the value (64) of λ, we find again that α has only a second-order variation, and we obtain a new value of the "continuous damping" β:

$$\boxed{\frac{\beta}{2m} = \frac{\omega^2(\nu - 1)\Delta x}{2c} - \frac{\omega^2[2(\theta - \phi)\nu - 1]\Delta x}{2c\left[1 + \frac{\rho_0 L}{m}\left(1 + \frac{m^2\omega^2}{\rho_0^2 c^2}\right)\right]} \ .} \tag{90}$$

This equation is again very close to (73). Naturally, it coincides with (73) if we take $\phi = 0$, but it gives a different prediction for β if $\phi \neq 0$. In order to test this expression, we performed four numerical simulations, with $\theta = 0$ or 1 and $\phi = 0$ or 1 (and $\nu = 0.45$). The results are presented in the following table:

(θ, ϕ)	$(0,0)$	$(0,1)$	$(1,0)$	$(1,1)$
Numerical damping	- 1.326	+ 0.250	- 2.917	- 1.318
Predicted damping	- 1.321	+ 0.181	- 2.823	- 1.321

Table 1: Numerically observed and analytically predicted values of the damping factor β for the (θ, ϕ)-scheme.

We again have a very good agreement between the prediction and the results of the simulations. Relative errors between the analytically predicted and the numerically observed damping are less than 3%, except in the case $(\theta, \phi) = (0, 1)$ (in this case, the absolute error between the prediction and the numerical value of β remains small, but the relative error is larger because β itself is rather small). Thus, the analytical prediction (90) of the numerical damping appears to be quite satisfactory for the class of schemes under consideration.

Remark 4: Notice also on Table 1 that the simulation with $(\theta, \phi) = (0, 1)$ ran unstable: $\beta > 0$. We see here that the method for the *coupled* system might be unstable, although the fluid scheme in itself operates under stable conditions ($\nu < 1$). This point is investigated in our next report [14]. •

6.2 Second-order accurate schemes

So far, we have restricted our attention to first-order accurate schemes for the fluid approximation. In this section, we turn to a second-order accurate explicit scheme and analyse the influence of this modification on our analytical predictions of the stiffness and damping parameters α and β. We are going to use the modified equation analysis.

Let us therefore assume that we use for the integration of (9) a scheme which is second-order accurate in both time and space (such as the Lax-Wendroff, or second-order upwind, or leap-frog schemes...). Then, the modified equation writes, up to second-order accuracy:

$$W_t + \begin{pmatrix} 0 & 1 \\ c^2 & 0 \end{pmatrix} W_x = \lambda \begin{pmatrix} 0 & 1 \\ c^2 & 0 \end{pmatrix} W_{xxx} \ , \tag{91}$$

with $\lambda = O(\Delta x^2)$ (for instance, $\lambda = \dfrac{\Delta x^2}{6}(\nu^2 - 1)$ for the leap-frog and Lax-Wendroff schemes; see [1]).

In order to reach also second-order accuracy for the structure, we use the scheme (56)-(58) with $\theta = 1/2$. Indeed, when $\theta = 1/2$, in full agreement with our previous observations on the meaning of θ and the interpretation of V_p^n (see Section 5), we can rewrite (56)-(58) as:

$$\Phi_{N+1/2}^n = \begin{pmatrix} \rho_0 V_p^* \\ c^2 \Delta \rho_N^n \end{pmatrix} , \tag{92}$$

$$V_p^* = \frac{V_p^{n-1/2} + V_p^{n+1/2}}{2} , \quad m\frac{V_p^{n+1/2} - V_p^{n-1/2}}{\Delta t} = c^2 \Delta \rho_N^n , \tag{93}$$

and this scheme is obviously second-order accurate.

Then, we can easily conduct the modified equation analysis. Using (40), we can show that the equation for z still takes the form (75), with $a = cz(\lambda z^2 - 1)$. The asymptotic expansions then give:

$$\boxed{\alpha = -m\omega^2 - 2m\frac{\omega^5 c^3 L}{\dfrac{\omega L}{c} + \dfrac{\rho_0 m c \omega}{\rho_0^2 c^2 + m^2 \omega^2}}\lambda + O(\lambda^2) ,} \tag{94}$$

$$\boxed{\frac{\beta}{2m} = O(\lambda^2) .} \tag{95}$$

We see that the dispersion parameter λ produces a perturbation of the second order in Δx in the pulsation (like the diffusion μ) and a negligible fourth order perturbation on the damping.

6.3 Implicit time integration schemes

In this section, we consider the temporal integration of our acoustic model with implicit schemes. We will still use the coupled eigenvector analysis to predict the spatial and temporal pulsations.

6.3.1 Presentation of the schemes

We now present a staggered implicit scheme for the solution of our model problem. For the time step from t^n to t^{n+1}, we first compute the evolution of the fluid, and then the evolution of the structure in a second step. For the fluid integration, we use predictions of the evolution of the structure based on its state at time t^n (but the state of the structure at t^{n+1} is not available in this fluid step); on the other hand, for the structural integration, we can use the state of the fluid at time t^{n+1}.

In the preceding sections (except in Section 6.2), we have used a classical first-order accurate explicit upwind scheme. The flux at the cell interfaces in the fluid was given by:

$$\Phi_{i+1/2}^n = A^+ W_i^n + A^- W_{i+1}^n , \tag{96}$$

where $A^{\pm} = \frac{1}{2}\begin{pmatrix} \pm c & 1 \\ c^2 & \pm c \end{pmatrix}$, and the boundary fluxes were given as:

$$\Phi^n_{1/2} = \begin{pmatrix} 0 \\ c^2\Delta\rho^n_1 - c\Delta(\rho u)^n_1 \end{pmatrix} \ , \quad \Phi^n_{N+1/2} = \begin{pmatrix} \rho_0 V^*_p \\ c^2\Delta\rho^* \end{pmatrix} \ , \tag{97}$$

with (from (82)):

$$V^*_p = V^n_p + \frac{c^2\theta\Delta t}{m}\Delta\rho^n \ , \tag{98}$$

$$\Delta\rho^* = \Delta\rho_N{}^n + \frac{\phi\Delta t}{\Delta x}\left(A^+W^n_{N-1} + A^-W^n_N - \rho_0 V^*_p\right) \ . \tag{99}$$

All fluxes we just wrote are basically explicit. We consider from now on that, as far as the fluid is concerned, we use hybrid explicit-implicit fluxes obtained by substituting:

$$F^n \longrightarrow (1-\chi)F^n + \chi F^{n+1} \ . \tag{100}$$

Moreover, in order to consider all implicit possibilities since the fluid's state F^{n+1} is already known, we introduce a new updating scheme for the piston. Instead of (57), we will write:

$$m\frac{V^{n+1}_p - V^n_p}{\Delta t} = c^2\left((1-\psi)\Delta\rho^n + \psi\Delta\rho^{n+1}\right) \ . \tag{101}$$

For the fluid alone, this scheme is unconditionally stable when $\chi \geq 1/2$. If $\chi < 1/2$, the hybrid scheme is stable under the condition:

$$\nu \leq \frac{1}{1-2\chi} \ . \tag{102}$$

6.3.2 Coupled eigenvector analysis

We present again the main outlines of the computation. Writing implicit fluxes instead of explicit ones in the conservation equations for a standard cell gives instead of (64) the new relation:

$$\frac{A^{n+1}}{A^n} = \frac{B^{n+1}}{B^n} = \frac{1 + (\chi-1)\dfrac{c\Delta t}{\Delta x}\left(1 - e^{-z\Delta x}\right)}{1 + \chi\dfrac{c\Delta t}{\Delta x}\left(1 - e^{-z\Delta x}\right)} = \lambda \ . \tag{103}$$

The conservation equation for the first cell again gives equations (66) and (67). Lastly, the conservation equation for the last cell gives back (after some long calculations) equations (85) and (86). Then, using the new equations (101) and (103), we find a new equation for z:

$$\boxed{\left[\frac{\rho_0\Delta x}{m\left(e^{-z\Delta x} - 1\right)} + e^{-z\Delta x} - 1 + \frac{\rho_0 c\Delta t}{m}\left(\theta + \psi - 1\right)\right]\left[k_d e^{zx_N} + e^{-zx_N}\right] = e^{z(x_N - \Delta x)} - e^{-zx_N}} \ . \tag{104}$$

Now, we want to study this equation when Δx is considered as very small (compared with c/ω). But we can no longer consider Δt as small since the time step Δt is not limited by any CFL-like condition (if we choose $\chi \geq 1/2$).

First we must notice that the expansion (88) for k_d is no longer valid, since Δt may be not small. In order to avoid any boundary artefact at spatial convergence, we would like to have:

$$\lim_{\Delta x \to 0} k_d = 1 \ . \tag{105}$$

This condition was automatically met for explicit schemes. For implicit schemes, the condition (105) will be satisfied if we take:

$$\boxed{\phi = 0 \ .} \tag{106}$$

With some easy computations, we find that z tends towards a limit z_1 when Δx tends to 0, with z_1 solution of:

$$z_1 \tanh(z_1 L) = -\frac{\rho_0}{m}\left(1 - z_1 c \Delta t(\theta + \psi - 1)\right) \ . \tag{107}$$

Thus, if we want the spatial and temporal pulsation to take a value independent of the time step, we have to take:

$$\boxed{\theta + \psi = 1 \ .} \tag{108}$$

If (108) holds, then $z_1 = z_0 = \pm\dfrac{i\omega}{c}$ with ω given by (26). We can now write the expansion of the solution z of (104) around z_0 in terms of Δx:

$$z = z_0 - \frac{\omega^2}{2c^2}\left[1 + \frac{\rho_0 L}{m}\left(1 + \frac{m^2\omega^2}{\rho_0^2 c^2}\right)\right]^{-1} \Delta x \ , \tag{109}$$

and we deduce the expansion of λ:

$$\lambda = \frac{1 + i(\chi - 1)\omega\Delta t}{1 + i\chi\omega\Delta t} - \frac{\omega^2 \Delta t}{2c}\frac{\left(1 - \left[1 + \dfrac{\rho_0 L}{m}\left(1 + \dfrac{m^2\omega^2}{\rho_0^2 c^2}\right)\right]^{-1}\right)}{\left(1 + i\chi\omega\Delta t\right)^2}\Delta x \ . \tag{110}$$

We have chosen here $z_0 = +\dfrac{i\omega}{c}$. If we had chosen the conjugate value for z_0, we would have found the conjugate value of λ. We see also that:

$$\lim_{\Delta x \to 0} \lambda = \frac{1 + i(\chi - 1)\omega\Delta t}{1 + i\chi\omega\Delta t} \ . \tag{111}$$

Recalling that the stiffness coefficient α is defined by $\alpha = -m|a|^2$, where a is chosen such that $\lambda = \exp(a\Delta t)$, we see that α will have a second-order variation from its unperturbed value $-m\omega^2$ if $\lambda = exp(\pm i\omega\Delta t) + O(\Delta t^2)$ (in the limit of Δx going to 0). From (111), this can be realized if we choose:

$$\boxed{\chi = \frac{1}{2} \ .} \tag{112}$$

With this choice, the stiffness and damping coefficients α and β have the following expansions:

$$\boxed{\alpha = -m\omega^2\left(1 - \frac{\omega^2\Delta t^2}{6} + O\left(\omega^3\Delta t^3\right) + O(\Delta x^2)\right) \ ,} \tag{113}$$

$$\boxed{\frac{\beta}{2m} = \frac{-\omega^2}{2c\left(1+\dfrac{\omega^2\Delta t^2}{4}\right)}\left(1-\left[1+\frac{\rho_0 L}{m}\left(1+\frac{m^2\omega^2}{\rho_0^2 c^2}\right)\right]^{-1}\right)\Delta x + O(\Delta x^2)\ .} \tag{114}$$

Let us make a few remarks on this last prediction. First, we see that β is always negative (and this point is clearly related with the unconditional stability of the hybrid explicit-implicit scheme when $\chi = 1/2$). Notice also that the free parameters θ and ψ (on which we have imposed the relation (108)) are not involved in the preceding analytical prediction for β.

The unconditional global stability of these coupled schemes makes it possible to choose the time step according to accuracy requirements. For instance, for $\Delta t = \dfrac{T}{25}$, $T = \dfrac{2\pi}{\omega}$ being the period of the system, the relation (113) predicts only a one percent error on the system pulsation α. However, numerical tests tend to show that the preceding predictions are not as accurate as expected. A possible explanation is that terms of higher order in Δx in (113) and (114) may not be negligible.

Remark 5: We see on (114) that the damping does depend on the time step, and more precisely that increasing Δt (with Δx small and fixed) decreases the damping (i.e. increases β towards 0). This is a somewhat surprising conclusion, since the dissipation error of implicit scheme usually increases with the time step. But we should keep in mind here that the dissipation error of our implicit scheme (which is given by $\mu = \dfrac{c\Delta x}{2}\left(1+(2\chi-1)\nu\right)$ is independent of Δt when $\chi = \dfrac{1}{2}$. •

7 Discussion and conclusions

In this section, we gather the conclusions of the preceding analyses, and show how their results can be used in order to reduce the overall numerical damping in the simulations of the model problem. Since our objective is to improve the numerical simulations of fluid-structure interactions in more general situations, we will try to extend our conclusions to more complex cases.

7.1 Prediction of the numerical damping

As a first general conclusion, we have recovered on our model problem some features of the numerical schemes which are commonly used in aeroelasticity. First, for schemes like (56)-(58), where a prediction of the speed of the structure is used for the time integration of the fluid, we found that the resulting numerical damping increases with the time lag θ between the fluid and the structure (i.e., $|\beta|$ increases with θ). On the opposite, for schemes like (81)-(82), where the pressure is predicted at the fluid-structure boundary, we proved that the numerical damping decreases with the delay in the prediction of the pressure (i.e., $|\beta|$ decreases with ϕ). Both results are illustrated on Figure 2, where we have presented the speed of the piston as function of time for four choices of the parameters θ and ϕ: the solid line, the dashed line and

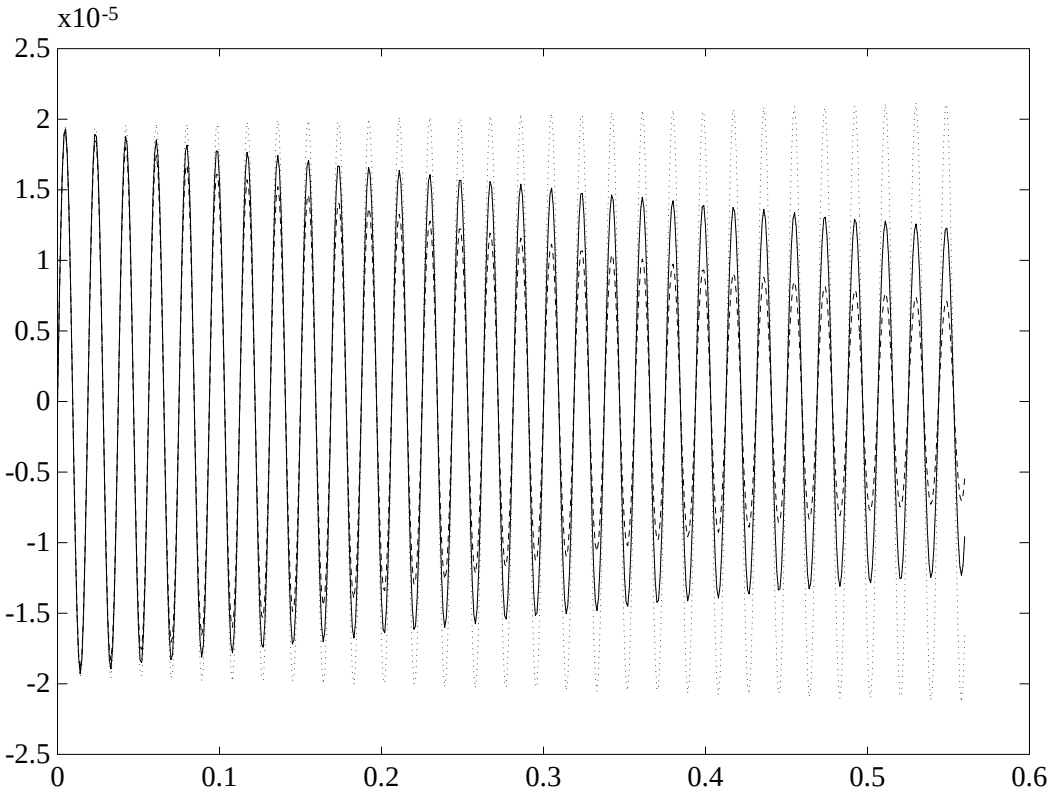

Figure 2: Piston speed as a function of time with different predictions using the (θ, ϕ) scheme.

the dotted line were respectively obtained with $(\theta, \phi) = (0, 0)$ and $(1, 1)$, with $(\theta, \phi) = (1, 0)$ and with $(\theta, \phi) = (0, 1)$. In full agreement with our analyses, we also notice on Figure 2 that changing the parameters θ and ϕ has a very little effect on the numerically observed pulsation.

We have then achieved our first goal: an accurate prediction of the global numerical damping. We have also explained why both predictions have opposite effects on the global damping. Moreover, the fact that this observation fully agrees with the general aeroelasticity know-how [12, 13] shows that analysing our linear model problem can be useful for understanding more general situations in aeroealsticity.

7.2 Compensation of the numerical damping

Now, as said in the introduction, we want to use our analytical predictions of the numerical results in order to reduce the numerical damping.

We will have to distinguish between two situations. Fluid-structure simulations can indeed be made in one of the two following opposite conditions: either one knows *a priori* a prediction of the pulsation and of the exact damping of the physical system, or no such prediction is available. In fact, an intermediate case could be considered, where upper and/or lower bounds for these values are known. In the following, we successively consider these cases and show

which conclusions can be drawn from the previous analyses.

7.2.1 Simulations with available predictions

Let us come back for a moment to our model acoustic problem, and perform some other numerical experiments, using the (θ, ϕ)-schemes of Section 6.1. Then, we can use our analytical prediction (90) to perform simulations where β is as small as possible: evaluating all terms in (90), we find that, for $\nu = 0.45$, β vanishes if $\phi - \theta = 0.88$. This was realized with the couples (0.12, 1.00) and (-0.88,0.00) for (θ, ϕ), and we actually obtained piston oscillations of fixed amplitude !

Therefore, when the pulsation and the damping of the physical system are known *a priori*, a correction of the scheme can be derived from our analytical predictions in order to recover the correct damping. For more general situations, this objective may be reached only approximately, by taking average values for the physical parameters (such as L, ρ_0..) involved in the analytical expression (90).

For our model problem, we also found an additional way of correcting the numerical scheme (but extending this second type of modification to multi-dimensional problem may be uneasy). We used a very simple scheme (with $\theta = 0$ and $\phi = 0$), but modified the piston time integration scheme as follows:

$$m \frac{V_p^{n+1} - V_p^n}{\Delta t} = c^2 \Delta \rho^n - \delta d \, V_p^n \ , \tag{115}$$

where δd is a small adaptable negative damping factor. Using either the modified equation or the coupled eigenvector analyses, it can be shown that the overall damping β vanishes if the artificial negative damping δd is taken equal to:

$$\delta d = -\frac{L \rho_0 \omega^2 \mu}{c^2} \left(1 + \frac{m^2 \omega^2}{\rho_0^2 c^2} \right) \ , \tag{116}$$

where μ is given by (29). The efficiency of this modification is illustrated on Figure 3, where we observe a nearly perfectly undamped numerical simulation.

Let us also emphasize that all methods presented above can be applied to cases where the piston is physically damped and/or linked to a spring, that is with non-zero coefficients d or k in (12). The major difference is that the exact pulsation ω is no longer given by (26), but is obtained from the complex solution z of:

$$\left(mcz + d + \frac{k}{zc} \right) \tanh(zL) = -\rho_0 c \ . \tag{117}$$

Remark 6: Following the same approach as above for the explicit (θ, ϕ)-scheme, when we used equation (90) in order to perform simulations with no global damping, let us now examine if we can eliminate the first-order damping term written in (114) for the implicit scheme of Section 6.3. Ideally, we would like to do this without losing the second-order accuracy on α shown in (113). Thus, we will relax the conditions (108) and (112) and set instead:

$$\chi = \frac{1}{2} + \gamma \ , \quad \theta + \psi = 1 + \delta \ , \tag{118}$$

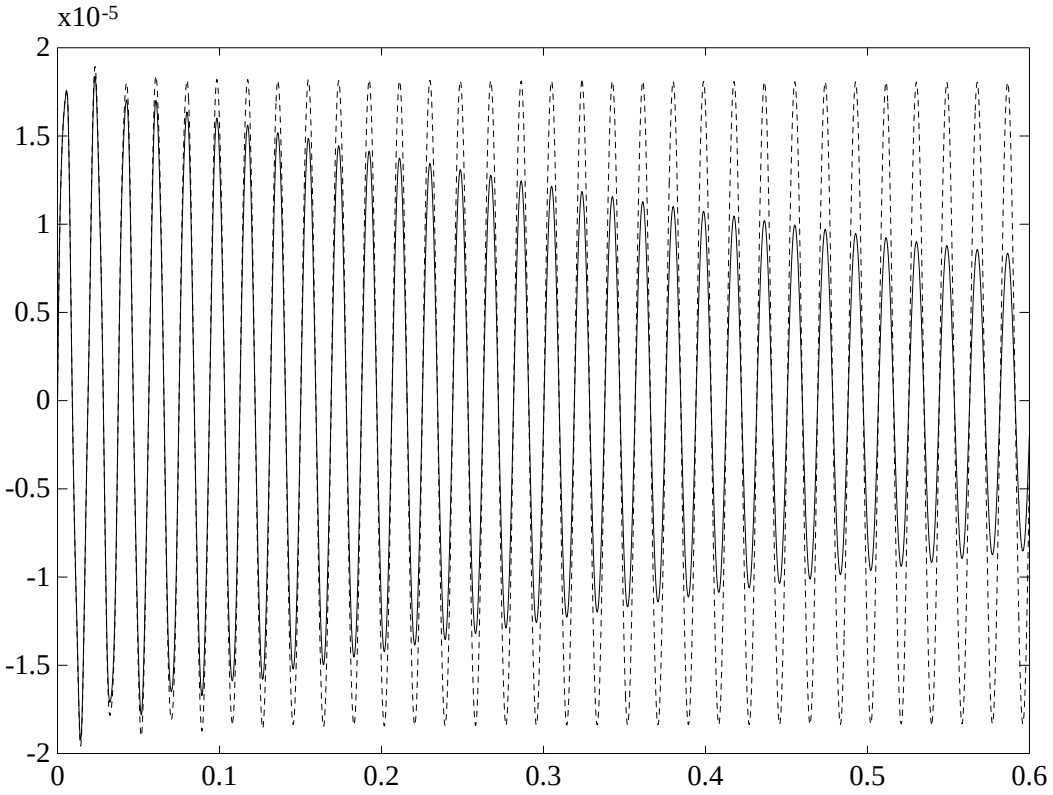

Figure 3: Piston's speed for two simulations : the undamped one is obtained with compensation via negative damping δd of the piston.

where γ and δ have to be chosen. Assuming that $c\delta\Delta t$ is small in (107), we obtain the following first-order expansions:

$$z = z_0 + D^{-1}\left[-\frac{\omega^2}{2c^2}\Delta x + \frac{\omega^2\Delta t}{c}\delta\right] \ , \tag{119}$$

where $D = 1 + \dfrac{\rho_0 L}{m}\left(1 + \dfrac{m^2\omega^2}{\rho_0^2 c^2}\right)$, and:

$$\lambda = \left[\frac{1 - i\omega\Delta t/2}{1 + i\omega\Delta t/2}\right]\left[\frac{1 + \omega^2\Delta t^2\left(\frac{1}{4} - \gamma\right) - D^{-1}\Delta t\left(\frac{\omega^2\Delta x}{2c}(D-1) + \omega^2\Delta t\delta\right)}{1 + \frac{\omega^2\Delta t^2}{4}}\right] \ . \tag{120}$$

We can now obtain the desired result:

$$\alpha = -m\omega^2\left(1 - \frac{\omega^2\Delta t^2}{6} + O\left((\omega\Delta t)^3\right) + O(\Delta x^2)\right) \ , \quad \beta = O(\Delta x^2) \ , \tag{121}$$

provided that we take:

$$\gamma = \delta = -\frac{\Delta x}{2c\Delta t} \ . \tag{122}$$

This result raises a problem: since γ is negative, we will have $\chi < 1/2$ from (118) and we may loose the unconditional stability of the scheme for the fluid; but this does not happen, since (118) and (122) imply that $\nu = \dfrac{1}{1-2\chi}$: in view of (102), we obtain an unconditionally (marginally) stable scheme. It seems therefore that we have found a close connection between our desire to suppress the global damping for the coupled system and the stability limit for the hybrid explicit-implicit scheme used in the fluid. •

7.2.2 Simulations with unavailable (accurate) prediction

In this part of the discussion, we assume that we do not dispose of predictions for the fundamental pulsation and damping of the physical system (this can be for instance the case for configurations where the masses of the fluid and of the structure are close to each other).

In such a case, most of the predictions presented in the preceding sections cannot be used. For our model problem with the physically undamped piston, we can however notice that the global damping factor β given by (73) can be made equal to zero (without using any information on the pulsation ω) by taking $\nu = 1$ and $\theta = 1/2$, which respectively produce no numerical damping in the fluid and in the structure. For the implicit scheme also, we can obtain zero damping, since no information on ω is used to choose γ and δ in (122). But in these two cases, these conclusions lead to use numerical schemes operating exactly at their stability limit, which cannot be useful for more general (nonlinear, multi-dimensional) situations. We therefore have to find some other methods for reducing the numerical damping.

In the case where the pulsation of the system can be bounded, the method (115) which introduces an artificial negative damping in the piston equation can provide help in decreasing the numerical damping in the simulation. Let us indeed call $\delta d(\omega)$ the right-hand side of (116) (notice that δd is a monotone decreasing function of ω). If we know *a priori* a lower bound

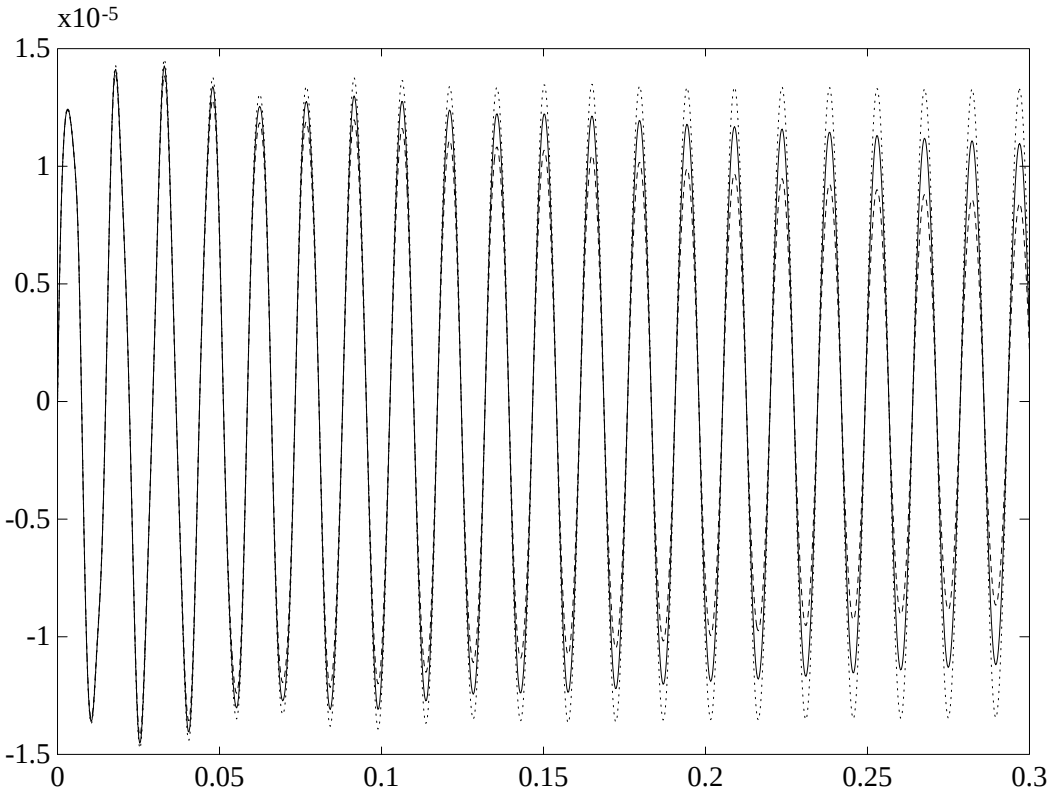

Figure 4: Piston speed for three compensation modes: no compensation (dashed line), compensation via negative damping δd based on the spring pulsation ω_s (solid line) or on the coupled system pulsation ω (dotted line).

$\omega \geq \Omega$ on the system pulsation ω, then we can use the equation (115) for the piston, with $\delta d = \delta d(\Omega)$: this is a safe way to obtain a better (less damped) simulation, with no risk of unstability.

As an example, consider the undamped piston with a spring (i.e., take $d = 0$ but $k > 0$ in (12)). The pulsation of the coupled system is then given by:

$$\left(\omega^2 - \omega_s^2\right) \tan(\frac{\omega L}{c}) = \frac{\omega \rho_0 c}{m} \ , \tag{123}$$

where $\omega_s = \sqrt{\frac{k}{m}}$ is the spring pulsation. In a case where the system pulsation ω is larger than the spring pulsation ω_s, we tried the above method, with $\delta d(\omega_s)$. The results are shown on Figure 4, where the improvement clearly appears.

Remark 7: Finally, other procedures based on energetic formulations can also be imagined (but their extensions to multiple dimensions are really not obvious). However, they can give interesting results for our model problem. Starting from the expression of the fluid energy per unit volum $\left(\frac{P}{\gamma - 1} + \frac{1}{2}\rho u^2\right)$, assuming that the evolution of the fluid is isentropic and using the expansions of P, u and ρ in terms of the perturbations $\Delta\rho$ and Δu, we find that the total

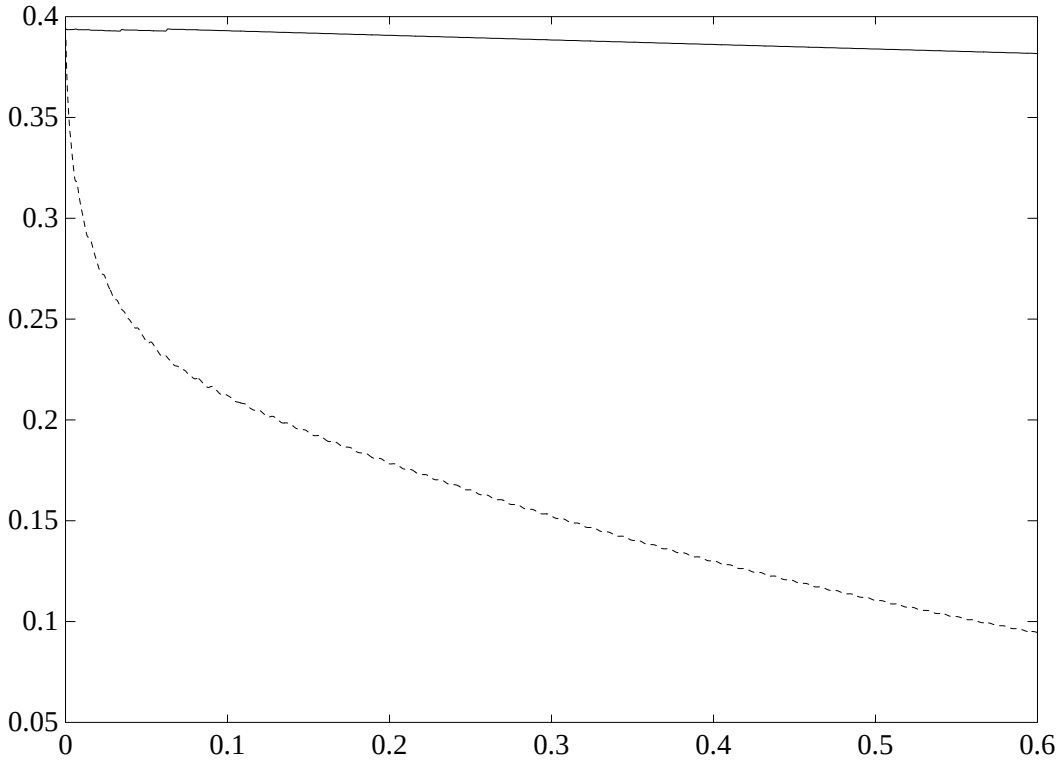

Figure 5: Total energy of the system during the simulation : the upper curve is obtained with a negative damping based on energy compensation, as in Remark 7.

energy in the system is given by:

$$E = \frac{1}{2\rho_0}\left(\int_0^L c^2\Delta\rho^2 + \rho_0^2\Delta u^2\right) + \frac{1}{2}m\dot{x}^2 \ . \tag{124}$$

The (constant) equilibrium energy has been omitted in the preceding equation. The reader will also notice that all first-order terms have disappeared in the expression of the total energy (these terms exactly cancel because the perturbations $\Delta\rho$, Δu and x are solutions of the linear system (9)-(12).

For a given spatial scheme in the fluid and given time integration schemes for the fluid and the piston, we can evaluate the variation of the total energy in terms of all computational values. For instance, for the first-order accurate explicit upwind scheme coupled with the explicit scheme (57), we obtain:

$$E^{n+1} = E^n - \frac{c\Delta t}{2\rho_0}\left(1 - \frac{c\Delta t}{\Delta x}\right)\sum_i \left(W_{i+1} - W_i\right)^t B \left(W_{i+1} - W_i\right) + O(\Delta t^2) \ , \tag{125}$$

where the symmetric positive definite matrix B is such that W^tBW is the discrete form of the integral term of (124).

Then, as we did in (115), we can add in the piston equation a negative damping δd evaluated at each time step in order to give back to ths system the amount of energy dissipated during

the current time step. This procedure has shown very interesting results in the one-dimensional model problem with an explicit time-integration scheme (see Figure 5). However, the negative damping had to switched off when the piston speed was too small (this term is basically given by the relation $\delta d\dot{x}^2 = \delta E$, where δE is the dissipated energy). Perturbations on the momentum balance of the system were also observed. Moreover, if the structure had not been reduced to a single point, a remaining question would have been to know where – on the structure – and how give back to the system the dissipated energy. •

7.2.3 Conclusions

The coupled problems which are to be investigated in realistic fluid-structure interactions problems are so complex that we need to examine simplified model problems in order to analyse in detail the behaviour of the numerical solution for the coupled system. For the one-dimensional model problem proposed in this report, we have derived efficient ways of analysing the overall effect of the numerical schemes on the pulsation and the amplitude of the system oscillations, and of compensating these effects by modifying the discrete formulations, for a wide class of numerical methods. There is good hope that several of these techniques can be useful for more general problems (although this conjecture still needs to be supported by more general numerical simulations, which we will undertake in a forthcoming work).

ACKNOWLEDGEMENTS:

We wish to thank our colleagues Charbel Fahrat, Loula Fezoui and Katherine Mer, with whom we had fruitful conversations during completion of this work.

The modeling part of this work was done while the third author was visiting CERMICS and INRIA, with support from DRET (under contract 92/322).

References

[1] D. A. ANDERSON, J. C. TANNEHILL & R. H. PLETCHER, "Computational fluid mechanics and heat transfer", Hemisphere, Mc Graw-Hill, (1984).

[2] J. T. BATINA, "Unsteady Euler airfoil solutions using unstructured dynamic meshes", AIAA J., **28**, pp. 1381-1388, (1990).

[3] R. L. BISPLIGHOFF, H. ASHLEY & R. L. HALFMAN, "Aeroelasticity", Addison-Wesley, Reading, (1957).

[4] C. J. BORLAND & D. P. RIZZETTA, "Nonlinear transonic flutter analysis", AIAA J. **20**, pp. 1606-1615, (1982).

[5] J. DONEA, S. GIULIANI & J. P. HALLEUX, "An arbitrary Lagrangian Eulerian finite-element method for transient dynamic fluid-structure interactions", Comp. Meth. Appl. Mech. Eng., **33**, pp. 689-723, (1982).

[6] C. FARHAT & T. Y. LIN, "Transient aeroelastic computations using multiple moving frames of reference", AIAA paper 90-3053-CP, (1990).

[7] G. P. GURUSWAMY, "Interaction of fluids and structures for aircraft applications", Comp. & Struct., **30**, pp. 1-13, (1988).

[8] A. HARTEN & J. M. HYMAN, "Self adjusting grid methods for one-dimensional hyperbolic conservation laws", J. Comp. Phys., **50**, pp. 235-269, (1983).

[9] K. ISOGAI & K. SUETSUGU, "Numerical calculation of unsteady transonic potential flow over three-dimensional wings with oscillating control surfaces", AIAA J., **22**, pp. 478-485, (1984).

[10] S. LANTERI, "Simulation d'écoulements aérodynamiques instationnaires sur une architecture S.I.M.D. massivement parallèle", *Ph.D. Thesis*, Université de Nice-Sophia-Antipolis, (1991).

[11] M. LESOINNE & C. FARHAT, *private commmunication.*

[12] K. C. PARK, C. A. FELIPPA & J. A. DE RUNTZ, "Stabilization of staggered solution procedures for fluid-structure interaction analysis", Computational methods for fluid-structure interaction problems, Belytschko & Geers eds., ASME Applied Mechanics Symposia Series, **26**, pp. 94-124, (1977).

[13] S. PIPERNO, "Numerical methods used in aeroelasticity simulations", CERMICS Report 92-5, (1992).

[14] S. PIPERNO & C. FAHRAT, "Time-integration schemes for a one-dimensional aeroelastic model-piston", *in preparation.*

[15] R. H. SCANLAN, "On the state of stability considerations for suspended-span bridges under wind", Proceedings IUTAM-IAHR Symposium, Karlsruhe, Germany, pp. 595-618, (1979).

[16] V. SHANKAR & H. IDE, "Aeroelastic computations of flexible configurations", Comp. & Struct., **30**, pp. 15-28, (1988).

[17] R. F. WARMING & F. HYETT, "The modified equation approach to the stability and accuracy analysis of finite-difference methods", J. Comp. Phys., **14**, (2), pp. 159-179, (1974).

Contents